

Quark Schwinger-Dyson Evaluation of the l_1, l_2 Coefficients in the Chiral Lagrangian.

F. J. Llanes-Estrada*

Depto. de Física Teórica I, Univ. Complutense. 28040 Madrid, Spain.

P. de A. Bicudo†

CFIF, Instituto Superior Técnico, Avda. Rovisco Pais 49001 Lisboa, Portugal

Using a systematic expansion of the quark-antiquark Bethe-Salpeter wavefunctions in the relativistic quark model and working to $O(P^4)$, in the chiral limit, we are able to derive theoretical expressions relating the coefficients of the chiral lagrangian l_1, l_2 to the underlying quark-antiquark wavefunctions and interaction kernels. This is accomplished by using a novel technique based on a Ward Identity for the quark-antiquark ladder kernel which greatly simplifies the required effort. Numerical evaluations are performed in two simple specific models.

I. INTRODUCTION.

It has traditionally been considered a triumph of theoretical physics when the parameters of an effective, low energy theory which correctly describe phenomena at a given scale can be related to those of an underlying, more fundamental scheme of thought which grounds it. Brilliant examples are Fritz London's explanation of the quantum nature of the Van der Waals forces [1] or the derivation of the atomic relativistic corrections as a consequence of the Dirac's equation for the electron. Low energy hadronic processes are interpreted with the aid of mainly two types of theories: nucleon-nucleon non relativistic interactions such as the Nijmegen [2] or Argonne [3] potentials, for the heavier hadrons, and relativistic chiral lagrangians [4] for the lightest components, the pions.

The deeper quark theories such as QCD or any microscopic models thereof pretend in principle to describe the totality of hadronic physics. They attempt to be complete descriptions of hadronic processes. Unfortunately, the complexity of many body hadronic calculations makes it forbidding to fully exploit the underlying scheme, and maintain the validity of the low energy effective theory.

As a consequence, an initial goal for the microscopic theory should be to reproduce in some limit the macroscopic models and to relate their parameters to its own set (hopefully smaller). In this paper we make the case for microscopic quark models inspired in QCD as generating the parameters of the chiral lagrangian. This lagrangian, describing the low energy behavior of a pion system, and being able to incorporate the coupling of pions to other mesons (as much as the low energy theorems of PCAC [5] do) is universal (in the sense that any theory with the same symmetries can be cast in its form) and provides a consistent derivative expansion in powers of the momentum and mass of any pions present in a sys-

tem, divided by a typical scale of the strong interactions.

Unfortunately, this derivative expansion has to incorporate new coefficients order by order. These new coefficients absorb the divergences of loops generated by the vertices of smaller order terms, and so their value is generally renormalized. Still, the common usage of this Lagrangian [6] proceeds by fitting this coefficients to some observable set at a given scale.

We show how these coefficients can be related systematically to quark level parameters in the planar approximation. This has been accomplished in the past for the simplest, $O(P^2)$ chiral lagrangian whose parameters are only two, in usual notation, M_π, f_π (the pion mass and decay constant). To this order, these two parameters are conventionally set to take their physical value. To the next order, the lagrangian contains six parameters, which generate the $O(P^4)$ vertices, l_1, l_2 , absorbing divergences in the 4 pion Green function, l_3, l_4 which absorb counterterms of the mass and axial current renormalizations, and finally M_π, f_π . The complete renormalization scheme is specified in [4]. The parameters M_π, f_π have long been accounted for by relativistic quark models [7, 8]. The l 's on the other hand have not been treated in quark models with non-contact interactions. We insist in the point that any theory which respects the $SU(2)_L \times SU(2)_R$ chiral symmetry breaking pattern, let it be a Nambu-Jona-Lasinio quark theory [9], a large N_c expansion [10], a string theory or any other exotic creation, can be cast in the form of the chiral lagrangian and the only difference between all of them is the numerical values of the l_i coefficients.

It is therefore of paramount importance to determine them from the theories which we believe correctly describe the physics at the GeV scale, in terms of quarks and antiquarks. Lattice determinations are making progress in that direction [11], but the Schwinger-Dyson equation formalism should provide an alternative determination in the near future. An interesting paper [12] exists where, at the lagrangian level, the action for a relativistic quark model is bosonized to obtain an effective meson lagrangian, used then to calculate pion-pion scattering lengths. We are going to theoretically extend this approach in two directions. First, we will start with the

*Electronic address: fllanes@fis.ucm.es

†Electronic address: bicudo@ist.utl.pt

most general chirally symmetric quark model, in which the pion is well described by a quark-antiquark pair after chiral symmetry breaking (encompassing in this way an ample spectrum of models) and by using their chiral properties, reduce the four pion Green's functions to a minimal set of diagrams. In this way, no bosonization is performed, and at all steps the way quark interactions arrange themselves to comply with the chiral theorems is explicitly visible. Second, comparing the result with the same calculation in a chiral lagrangian formalism, one can immediately read off the l_i coefficients of the chiral lagrangian in terms of diagrams which can numerically be calculated in the quark model. This rather technical numerical evaluation will be simplified in this work by confining ourselves to simple, finite models, although the numerical results will then be limited. The method used here has already successfully being exploited to demonstrate how this class of models comply with the Weinberg theorem in [13, 14, 15]. The Weinberg theorem was derived with an expansion to $O(P^2)$, $O(M_\pi^2)$. We now concentrate on the $O(P^4)$, $O(M_\pi^0)$ chiral lagrangian, that is, the only parameters are f_π , l_1 , and l_2 . We will perform the same expansion in the quark-antiquark diagrams and compare the results to read off l_1 , l_2 . The expansion will be carried out whenever possible in a Feynman diagram language to avoid lengthy expressions for the sake of readability. The rest of this paper is organized as follows: in section II we briefly settle the notation for our chiral perturbation theory discussion and remind the reader of a few well-known facts in this field. Section III settles the notation of the microscopic quark manipulations to follow and provides the reader with a useful chiral Ward Identity recently introduced [13], [14]. Section IV is the core of the paper and presents the reduction of the pion scattering amplitude, whereas the resulting diagrams are calculated in two simple models in section V. Some issues clarifying the normalization of the Bethe-Salpeter equation are relegated to the appendix.

II. CHIRAL LAGRANGIAN OF ORDER P^4 .

The macroscopic theory one generally writes down for pion fields alone is to lowest order the Non Linear Sigma Model. One can proceed by constructing, from the three pion fields, $\vec{\pi} = (\pi_1, \pi_2, \pi_3)$, a 4-vector normalized to one (this normalization is equivalent to eliminating the explicit σ degree of freedom from the Linear Sigma Model)

$$U = \left[\begin{array}{c} \sqrt{1 - \frac{\vec{\pi}^2}{F^2}} \\ \frac{\vec{\pi}}{F} \end{array} \right] \quad (1)$$

and then constructing Lorentz scalar, parity invariant terms. To $O(P^4)$ that lagrangian can be extended by terms which in the chiral limit ($m_q = 0$) have to be of the form [4]

$$\mathcal{L}^{(4)} = \frac{1}{F^4} (l_1(\vec{\pi}_{,\mu} \cdot \vec{\pi}^{\mu}) (\vec{\pi}_{,\nu} \cdot \vec{\pi}^{\nu}) + l_2(\vec{\pi}^{\mu} \cdot \vec{\pi}^{\nu}) (\vec{\pi}_{,\mu} \cdot \vec{\pi}_{,\nu})) \quad (2)$$

where the scalar product dots are in isospin space. This lagrangian is on shell, for massless pions (else the l_3 , l_4 counterterms should also be present) and contributes at tree level to the $O(P^4)$ pion-pion scattering amplitude, and it is this contribution which we aim to reproduce microscopically. In the chiral formalism, there are also one-loop contributions from the $O(P^2)$ lagrangian which we do not consider in this work, since our quark-level calculation will not be extended to meson loops. Therefore, to this level, it is fair to compare our results only with those obtained in chiral perturbation theory without meson loops. With this caveat in mind, the pion-pion scattering amplitudes are straightforwardly obtained. By using crossing symmetry, the different isospin channels can be related in terms of only one amplitude A :

$$T_{I=2} = A(t, s, u) + A(u, t, s) \quad (3)$$

$$T_{I=1} = A(t, s, u) - A(u, t, s)$$

$$T_{I=0} = 3A(s, t, u) + A(t, s, u) + A(u, t, s) .$$

This amplitude $A(s, t, u)$ can be obtained from the process $\pi_+\pi_- \rightarrow \pi_0\pi_0$. Due to the final state Bose symmetry, and in the chiral limit when the Mandelstam variables satisfy $s+t+u=0$, the most general amplitude of order P^4 containing the polynomials $s^2, t^2, u^2, st, su, tu$, reduces to $A_1 s^2 + A_2 (t-u)^2$. The coefficients obtained from the lagrangian (2) above yield

$$A^{(4)}(s, t, u) = \frac{1}{F^4} [(2l_1 + \frac{l_2}{2})s^2 + \frac{l_2}{2}(t-u)^2] . \quad (4)$$

A full discussion of this and related issues, for example the relation between f_π and F which we further ignore in this paper to the order we are working can be found in [4, 16].

III. NOTATION FOR QUARK MODELS AND CHIRAL WARD IDENTITIES.

A pion with momentum P couples in relativistic models to fermion lines whose momenta will be denoted by k, k' . In the massless quark limit, whenever $P=0$, then $k=k'$. We start by considering the bare fermion propagator from any standard quark theory,

$$S_0(k) = \frac{i}{\not{k} - m + i\epsilon} \quad (5)$$

and, after spontaneous chiral symmetry breaking mediated by a strong interaction [17], [18], the full fermion propagator parameterized as

$$S(k) = \frac{i}{A(k^2) \not{k} - B(k^2) + i\epsilon} \quad (6)$$

which we take to be a solution of the planar Rainbow Schwinger-Dyson equation

$$S(k)^{-1} = S_0(k)^{-1} - \int \frac{d^4 q}{(2\pi)^4} V^a S(k+q) V_a K(q) . \quad (7)$$

We further define the bare axial vertex which couples a quark-antiquark pair to a pseudoscalar current by means of the shorthand γ_A^a (notice that $m_u = 0 = m_d$ in the chiral limit employed in this paper):

$$\gamma_A^a = \frac{\sigma^a}{2}(-iP_\mu \gamma^\mu \gamma_5 + 2im_u \gamma_5) \quad (8)$$

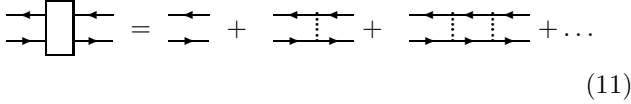
which satisfies

$$\gamma_A^a(k, k') = \frac{\sigma^a}{2}(S_0^{-1}(k)\gamma_5 + \gamma_5 S_0^{-1}(k')) \quad (9)$$

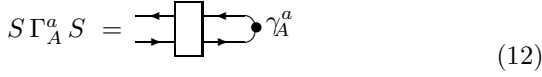
and the dressed axial vertex, dressed with a planar ladder Γ_A , given by

$$\Gamma_A^a(k, k') = \gamma_A^a(k, k') + \int V^a S(k_1 + q) \Gamma_A^a S(k_2 + q) V_a K(q) \quad (10)$$

or reconstructing the planar ladder expansion (in graphical form):



$$(10) \text{ takes the form} \quad (11)$$

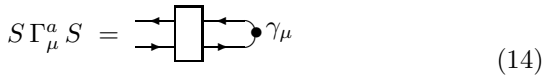


$$S \Gamma_A^a S = \dots \quad (12)$$

from which one can deduce the axial vector Ward Identity:

$$\Gamma_A^a(k, k') = \frac{\sigma^a}{2}(S^{-1}(k)\gamma_5 + \gamma_5 S^{-1}(k')) := \frac{\sigma^a}{2} \Gamma_A. \quad (13)$$

This is analogous to the abelian vector Ward-Takahashi Identity which in terms of the vertex Γ_μ defined by



$$S \Gamma_\mu S = \dots \quad (14)$$

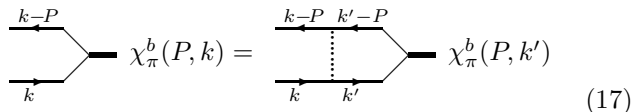
yields

$$i(k_\mu - k'_\mu) \Gamma_\mu(k, k') = S^{-1}(k') - S^{-1}(k). \quad (15)$$

Next we introduce the bound state formalism for quark-antiquark systems. To this end we remind the reader of the Bethe-Salpeter (BS) amplitude χ (see [7], [12]) for further details) which satisfies a homogeneous Bethe-Salpeter equation:

$$\chi^b(P, k) = \int V_a S(k' + \frac{P}{2}) \chi^b(P, k') S(k' - \frac{P}{2}) V_a K(k - k'). \quad (16)$$

or in graphical form:



$$(17)$$

Each incoming or outgoing pion in a particular process must contribute with one of these χ functions, which carry pseudoscalar quantum numbers by construction [19]. The BS amplitude for a particular pion depends on the total momentum of the pion P , and the momentum of its fermion component $k \pm P/2$. Notice that this equation is the homogeneous part of (10) above when we interpret the pion momentum P as $k - k'$ in the vertex definition.

Now let us deepen our study of the vertex Γ_A . From (13) can easily be seen that in the chiral limit ($m_q=0$),

$$\Gamma_A^a(k, k' = k) = 2iB(k^2)\gamma_5 \frac{\sigma^a}{2}, \quad (18)$$

in terms of the SD amplitude B solution of (7). Equations (16) and (10), homogeneous and not homogeneous, coincide when $\gamma_A = 0$. This is satisfied in the limit $m_q = 0$ when also $P = 0$ as can be seen explicitly from (9) and allows us to identify, up to a normalization constant, $\chi_\pi(P = 0, k)$ with $\Gamma_A(k, k' = k)$. This constant coincides with if_π , the pion decay constant in the chiral limit (the proof is sketched in appendix A) and finally entails, in combination with (18),

$$\chi_\pi^a(P = 0, k) = \frac{-i\Gamma_A^a(k, k' = k)}{f_\pi} = \frac{2B(k^2)}{f_\pi} \gamma_5 \frac{\sigma^a}{2}. \quad (19)$$

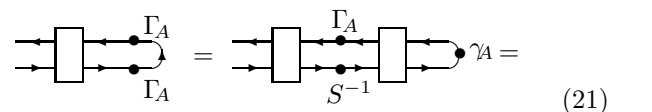
In [20] the proof was given why this BS amplitude, in connection with the Axial Vector Ward Identity makes the pion a Goldstone boson. In terms of our notation this has been rewritten in [14].

This discussion suggests a strategy to systematically organize the corrections to the chiral, low momentum limit, in an analogous fashion to that used in Chiral Perturbation Theory. Since the vertex Γ_A and diagrams constructed thereof satisfy interesting Chiral identities, let us define

$$\chi^a(P, k) = \frac{-i\Gamma_A^a(P, k) + \Delta^a(P, k)}{f_\pi} \quad (20)$$

where the function $\Delta(P, k)$ so introduced can be expanded in a Taylor series for low P . This expansion will organize the momentum corrections to any diagram. One will first use the chiral results for Γ_A , which will provide one with exact low energy theorems, and the numerical corrections as P is increased can then be expressed as overlaps of Δ functions.

We do not yet specify the color, spin, flavor or momentum structure of the interaction kernel and vertices $V_a V^a K(q)$, except for one property: it must be chiral symmetry preserving, that is, V commutes with γ_5 . This guarantees the satisfaction of the following Chiral Ward Identity (also discussed in [13], [14]) which proved essential:



$$(21)$$

or, for a general vertex not necessarily pseudoscalar:

(22)

This identity allows the reduction of terms with two axial vertices and is the core of the present calculation. (We remark that $S^{-1}S = I$ is introduced in (21) and S completes the ladder in eq. (11) leaving the explicit S^{-1} .)

A. Further Ladder Properties.

We start by observing that the pseudoscalar ladder can be Laurent-expanded around its pion pole. Keeping only the first term, containing the pole, one obtains:

(23)

where

(24)

(in the calculations contained in this paper, $m_\pi^2 = 0$.) Combining this together with the definition of Δ in eq. (20) one can use

(25)

The ladder can also be expanded in powers of the external momentum: starting from the geometrical series (11) and expanding all propagators, then resumming when possible, we can show that in analogy with the matrix relations

$$\left(\frac{1}{1-y}\right)' = \left(\frac{1}{1-y}\right) y' \left(\frac{1}{1-y}\right)$$

$$\left(\frac{1}{1-y}\right)'' = 2 \left(\frac{1}{1-y}\right) y' \left(\frac{1}{1-y}\right) y' \left(\frac{1}{1-y}\right) + \left(\frac{1}{1-y}\right) y'' \left(\frac{1}{1-y}\right)$$

one has

(26)

where the following momentum expansion of the propagators is meant by the super indices ⁽¹⁾, ⁽²⁾

$$S(q + P/2)|_{P=0} = \frac{A \not{q} + B}{A^2 q^2 - B^2} \quad (27)$$

$$\partial^\mu S(q + P/2)|_{P=0} = \gamma_\mu \frac{A/2}{A^2 q^2 - B^2} + q_\mu \left(\frac{A' \not{q} + B'}{A^2 q^2 - B^2} - \frac{(A \not{q} + B)(A^2 + 2q^2 AA' - 2BB')}{(A^2 q^2 - B^2)^2} \right) \quad (28)$$

$$\begin{aligned} \partial^\mu \partial_\mu S(q + P/2)|_{P=0} &= \frac{\not{q} A'}{A^2 q^2 - B^2} - \frac{A^2 + 2q^2 AA' - 2BB'}{(A^2 q^2 - B^2)^2} (\not{q} A + 2q^2 (\not{q} A' + B')) \\ &+ 2q^2 \left[\frac{A'' \not{q} + B''}{2(A^2 q^2 - B^2)} + \frac{A \not{q} + B}{(A^2 q^2 - B^2)^2} \left(\frac{(A^2 + 2q^2 AA' - 2BB')^2}{A^2 q^2 - B^2} - (2AA' + q^2 (A')^2 + q^2 AA'' - (B')^2 - BB'') \right) \right] \\ &+ \frac{2}{(A^2 q^2 - B^2)^2} [(A' \not{q} + B')(A^2 q^2 - B^2) - (A \not{q} + B)(A^2 + 2q^2 AA' - 2BB')] \end{aligned} \quad (29)$$

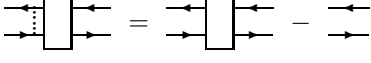
The last diagram in (26) contains an annoying explicit

rung of the interaction. This can be eliminated at the

cost of adding a diagram to any expression where it appears: in analogy with

$$\frac{y}{1-y} = \frac{1}{1-y} - 1$$

one can use

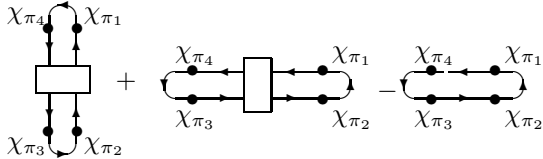


$$(30)$$

IV. PION-PION SCATTERING

A. Generalities.

The pion scattering amplitude with the Bethe-Salpeter and planar approximations can be derived from the following Feynman diagrams:



$$(31)$$

where the first two terms provide all possible planar topologies, but upon substitution of (11) their zeroth order is seen to be double counted, hence we subtract it. The two approximations involved are: first, coupling of the pion to higher Fock space states is not considered and second, only planar diagrams are utilized. It was shown, using the axial Ward Identity, that these two approximations are consistent within the Schwinger-Dyson method in the rainbow approximation for the fermion mass generation and in the ladder approximation for the bound state equation [13, 14]. This is also consistent with past work [21] on resonance exchange, and is equivalent to the lowest order in a $1/N_c$ expansion. Reduction of this combination of Feynman diagrams to $O(p^4)$, $O(M_\pi^0)$ is our goal. The calculations in this section will treat the P 's as incoming momenta. Matching the dummy P_j to the incoming q_{i1} , q_{i2} and outgoing q_{o1} , q_{o2} physical pion momenta leads to 6 different permutations, namely

$$(P_1, P_2, P_3, P_4) = \begin{pmatrix} (q_{i1}, q_{i2}, -q_{o2}, -q_{o1}) \\ (q_{i1}, q_{i2}, -q_{o1}, -q_{o2}) \\ (q_{i1}, -q_{o1}, -q_{o2}, q_{i2}) \\ (q_{i1}, -q_{o2}, -q_{o1}, q_{i2}) \\ (q_{i1}, -q_{o1}, q_{i2}, -q_{o2}) \\ (q_{i1}, -q_{o2}, q_{i2}, -q_{o1}) \end{pmatrix}, \quad (32)$$

where the first momentum is fixed to avoid double counting by rotational symmetry of the π - π scattering amplitude (31).

We concentrate on $A(s, t, u)$, the amplitude for $\pi_+ \pi_- \rightarrow \pi_0 \pi_0$, and use the following isospin wavefunctions

$$\pi_+ = \frac{1}{2}(\sigma_1 + i\sigma_2) \quad (33)$$

$$\pi_- = \frac{1}{2}(-\sigma_1 + i\sigma_2)$$

$$\pi_0 = \frac{1}{\sqrt{2}}\sigma_3.$$

From them follow the traces

$$Tr(\pi_+ \pi_- \pi_0 \pi_0) = -\frac{1}{2} \quad (34)$$

(which multiplies the four first permutations in (32) above where the two charged pions are adjacent) and

$$Tr(\pi_+ \pi_0 \pi_- \pi_0) = \frac{1}{2} \quad (35)$$

(multiplying the last two permutations in (32) where the two charged pions are in opposite corners of the amplitude).

Finally the Mandelstam variables in the chiral limit satisfy

$$\begin{aligned} s &= 2q_{i1}q_{i2} = 2q_{o1}q_{o2} \\ t &= -2q_{i1}q_{o1} = -2q_{i2}q_{o2} \\ u &= -2q_{i1}q_{o2} = -2q_{i2}q_{o1}. \end{aligned} \quad (36)$$

Since isospin has been factored out, we can ignore it in the rest of the calculation. Instead of working with Γ_a we employ Γ as defined in eq. (13). Accordingly, we define

$$\chi^a := \frac{\sigma^a}{\sqrt{2}}\chi \quad (37)$$

to yield the normalized isospin wavefunctions in (33) and the normalization for χ , Γ_A will be

$$\chi = \frac{-i\Gamma_A + \Delta}{\sqrt{2}f_\pi}. \quad (38)$$

We now start evaluating the Feynman amplitude in terms of the P 's. Start by employing (38) to treat the product of four BS amplitudes:

$$\chi_{\pi_1} \chi_{\pi_2} \chi_{\pi_3} \chi_{\pi_4} = \quad (39)$$

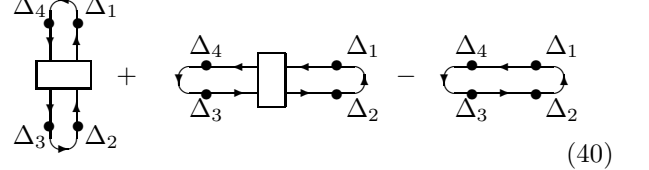
$$\begin{aligned} &\left(\frac{1}{\sqrt{2}f_\pi}\right)^4 \left(\frac{\Gamma_1}{i} + \Delta_1\right) \left(\frac{\Gamma_2}{i} + \Delta_2\right) \left(\frac{\Gamma_3}{i} + \Delta_3\right) \left(\frac{\Gamma_4}{i} + \Delta_4\right) \\ &= \left(\frac{1}{\sqrt{2}f_\pi}\right)^4 \left(\Delta_1 \Delta_2 \Delta_3 \Delta_4 + \frac{\Gamma_1}{i} \Delta_2 \Delta_3 \Delta_4 + \text{perm.}\right) + \dots \end{aligned}$$

where the omitted terms, contain an increasing number of powers of Γ . Next we proceed to a term by term analysis of this expansion, further explained in the paper [14].

B. Contribution with 4- Δ s.

The term with four Δ 's is model dependent and no chiral properties can be used to simplify it, since it contains corrections to the BS pion wavefunction beyond the zero momentum limit. Without evaluating it explicitly in a particular model yet (but see later), we can parameterize it. To the order m^0 we work here, for on-shell pions, $P_i^2 = 0$ for all i . Therefore, the 4- Δ diagrams can only be a combination of products of different momenta, $P_i P_j$. But to order P^4 , since each Δ brings at least one momentum power (the zeroth power is accounted for already in Γ), only combinations of the type $(P_1 P_2)(P_3 P_4)$, $(P_1 P_4)(P_2 P_3)$, $(P_1 P_3)(P_2 P_4)$ can appear. The coefficients of the first two terms have to be equal because of the cyclic symmetry of eqn. (31) The coefficient of the last term is in general independent.

In terms of fictitious momenta, all flowing into the diagram, whose conservation law is $P_1 + P_2 + P_3 + P_4 = 0$, we obtain



$$= 3d_1(P_1 \cdot P_2 \ P_3 \cdot P_4 + P_1 \cdot P_4 \ P_2 \cdot P_3) + 3d_2 P_1 \cdot P_3 \ P_2 \cdot P_4 \ . \quad (40)$$

The two numbers d_1, d_2 contain the non-trivial information in this diagram. We have explicitly pulled out the color factor (3 as will be shown shortly) from the d 's, which contain in this way only momentum and spin (since flavor will be dealt with at the end when the external legs are matched to the physical particles).

The third term in (40), to order 4 in momentum, with no ladder, is simply a wavefunction overlap given by the usual Feynman rules (notice an extra (-1) will be due to the fermion loop)

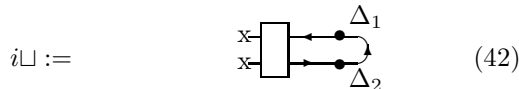
$$- \int \frac{d^4 q}{(2\pi)^4} \left(\frac{i}{A^2 q^2 - B^2} \right)^4 \text{Tr} \left[\Delta^{(1)}(P_1, q)(A \not{q} + B) \Delta^{(1)}(P_4, q)(A \not{q} + B) \Delta^{(1)}(P_3, q)(A \not{q} + B) \Delta^{(1)}(P_2, q)(A \not{q} + B) \right] \quad (41)$$

The Dirac traces can easily be computed with FORM. The integral is then reduced by using tensor identities like

$$\int F(q^2) q^\mu q^\nu q^\rho q^\sigma = \frac{g^{\mu\nu} g^{\rho\sigma} + g^{\mu\rho} g^{\nu\sigma} + g^{\mu\sigma} g^{\nu\rho}}{24} \int q^4 F(q^2)$$

to a one dimensional expression which can then be numerically evaluated once a specific model (and hence Bethe-Salpeter wavefunctions) is chosen. Notice that this simple momentum routing is correct only to order P^4 .

The first and second diagram in (40) contain a ladder. A simple way to calculate them is to write an integral equation for the object



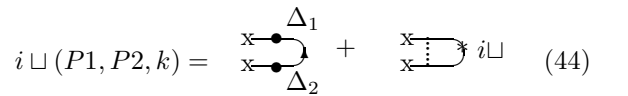
$$i\sqcup := \quad (42)$$

whose most general expansion up to second order in the

external pion momenta is

$$\sqcup := \sqcup_0(k^2) P_1 \cdot P_2 + \sqcup_1(k^2) k \cdot P_1 \ k \cdot P_2 + \sqcup_2(k^2) P_1 \cdot P_2 \not{k} + \sqcup_3(k^2) k \cdot P_1 \ k \cdot P_2 \not{k} + \sqcup_4(k^2) k \cdot P_2 \not{k} + \sqcup_5(k^2) k \cdot P_1 \not{k} + \sqcup_6(k^2) k \cdot P_2 \not{k} + \sqcup_7(k^2) k \cdot P_1 \not{k} + \sqcup_8(k^2) \not{k} + \sqcup_9(k^2) \not{k} \not{k} \quad (43)$$

The functions \sqcup_i are obtained by projecting this linear integral equation (analogous to the Bethe-Salpeter equation)



$$i\sqcup(P1, P2, k) = \quad + \quad i\sqcup \quad (44)$$

with the matrix projectors $I, \not{k}, \not{k} \not{P}_1, \dots, \not{k} \not{P}_1 \not{P}_2$, which provides us with a linear system of eight integral equations for the \sqcup_i . Defining a convenient quantity $D := 2k \cdot P_1 \ k \cdot P_2 - k^2 P_1 \cdot P_2$ the projections are

$$\begin{aligned} 4D(P_1 \cdot P_2 \sqcup_0 + k \cdot P_1 \ k \cdot P_2 \sqcup_1) &= \text{Tr}[(2D - 2k \cdot P_1 \not{k} \not{P}_2 + q^2 \not{P}_1 \not{P}_2) \sqcup] \\ 4D(P_1 \cdot P_2 \sqcup_2 + k \cdot P_1 \ k \cdot P_2 \sqcup_3) &= \text{Tr}[(-2P_1 \cdot P_2 \not{k} + 2k \cdot P_2 \not{P}_1 + \not{k} \not{P}_1 \not{P}_2) \sqcup] \\ 4P_1 \cdot P_2 D k \cdot P_2 \sqcup_4 &= \text{Tr}[(2k \cdot P_2 \ P_1 \cdot P_2 \not{k} - 2(k \cdot P_2)^2 \not{P}_1 + D \not{P}_2 - k \cdot P_2 \not{k} \not{P}_1 \not{P}_2) \sqcup] \end{aligned} \quad (45)$$

$$\begin{aligned}
4P_1 \cdot P_2 Dk \cdot P_1 \sqcup_5 &= Tr[(D \not{P}_1 - 2(k \cdot P_1)^2 + k \cdot P_1 \not{k} \not{P}_1 \not{P}_2) \sqcup] \\
4P_1 \cdot P_2 Dk \cdot P_2 \sqcup_6 &= Tr[(P_1 \cdot P_2 \not{k} \not{P}_2 - k \cdot P_2 \not{P}_1 \not{P}_2) \sqcup] \\
4P_1 \cdot P_2 Dk \cdot P_1 \sqcup_7 &= Tr[(-2k \cdot P_1 P_1 \cdot P_2 + P_1 \cdot P_2 \not{k} \not{P}_1 + k \cdot P_1 \not{k} \not{P}_1 \not{P}_2) \sqcup] \\
4P_1 \cdot P_2 D \sqcup_8 &= Tr[(k^2 P_1 \cdot P_2 - k \cdot P_2 \not{k} \not{P}_1 + k \cdot P_1 \not{k} \not{P}_2 - k^2 P_1 \not{P}_2) \sqcup] \\
4P_1 \cdot P_2 D \sqcup_9 &= Tr[(P_1 \cdot P_2 \not{k} - k \cdot P_2 \not{P}_1 + k \cdot P_1 \not{P}_2 - \not{k} \not{P}_1 \not{P}_2) \sqcup]
\end{aligned}$$

and the inhomogeneous part of the equation can easily be written down from the first RHS diagram in (44). Once the equation for \sqcup is solved in a computer, the diagram can be closed from the left to give

$$\begin{array}{c} \Delta_4 \\ \bullet \\ \Delta_3 \end{array} \bullet i \sqcup_{1,2} \quad (46)$$

and calculated as a simple integral. Here the color factor of 3 in (40) can be easily seen, since all three vertices are color singlets and carry $\delta_{cc'}$ in color space..

C. Contribution with $\Gamma - 3\Delta$.

We will reduce the $3-\Delta$ contribution fixing the indices $\Gamma_4 \Delta_1 \Delta_2 \Delta_3$ (the other permutations can at the end be easily generated). Employing (25) in

$$\begin{array}{c} \Gamma_4 \\ \bullet \\ \Delta_3 \end{array} \begin{array}{c} \Delta_1 \\ \bullet \\ \Delta_2 \end{array} + \begin{array}{c} \Gamma_4 \\ \bullet \\ \Delta_3 \end{array} \begin{array}{c} \Delta_1 \\ \bullet \\ \Delta_2 \end{array} - \begin{array}{c} \Gamma_4 \\ \bullet \\ \Delta_3 \end{array} \begin{array}{c} \Delta_1 \\ \bullet \\ \Delta_2 \end{array} \quad (47)$$

(in the first diagram fix $j = 3$ to substitute (25), in the second diagram employ $j = 1$) to obtain

$$\begin{aligned}
& \left(\frac{\sqrt{2}f_\pi \chi_3}{c_3} - \frac{\gamma_{A3}}{i} \right) \begin{array}{c} \Gamma_4 \\ \bullet \\ \Delta_3 \end{array} \begin{array}{c} \Delta_1 \\ \bullet \\ \Delta_2 \end{array} S^{-1} + \\
& \left(\frac{\sqrt{2}f_\pi \chi_1}{c_1} - \frac{\gamma_{A3}}{i} \right) \begin{array}{c} S^{-1} \\ \bullet \\ \Gamma_4 \end{array} \begin{array}{c} \Delta_2 \\ \bullet \\ \Delta_3 \end{array} - \\
& \begin{array}{c} \Gamma_4 \\ \bullet \\ \Delta_3 \end{array} \begin{array}{c} \Delta_1 \\ \bullet \\ \Delta_2 \end{array} \quad (48)
\end{aligned}$$

Next one can apply (22) to the single Γ appearing in this expression to generate, after some simple manipula-

tions:

$$\begin{aligned}
& \gamma_5 \left(\frac{\sqrt{2}f_\pi \chi_3}{c_3} - \frac{\gamma_{A3}}{i} \right) \begin{array}{c} \Delta_1 \\ \bullet \\ \Delta_2 \end{array} + \\
& \left(\frac{\sqrt{2}f_\pi \chi_1}{c_1} - \frac{\gamma_{A3}}{i} \right) \gamma_5 \begin{array}{c} \Delta_2 \\ \bullet \\ \Delta_3 \end{array} \quad (49)
\end{aligned}$$

From this expression, the two terms with c_j are zero in the chiral limit (as appropriate to this paper). The c_j 's diverge for low energies in the chiral limit: they contain the pseudoscalar ladder pole. But in this diagrams, the object to the right of the ladder contains a product of 2 Δ 's, each of negative parity, the result carrying positive parity. By the symmetry breaking pattern of the theory, no massless scalar, pseudovector or tensor meson pole can make the ladder divergent at low momentum. Therefore the terms with c_j can be discarded and we have to consider only (substituting $\gamma_A = \frac{P}{i} \gamma_5$, good in the chiral limit):

$$\frac{i}{(\sqrt{2}f_\pi)^4} \not{P}_3 \begin{array}{c} \Delta_1 \\ \bullet \\ \Delta_2 \end{array} - \frac{i}{(\sqrt{2}f_\pi)^4} \not{P}_1 \begin{array}{c} \Delta_2 \\ \bullet \\ \Delta_3 \end{array} \quad (50)$$

Therefore our next problem is to evaluate diagrams such as:

$$\begin{aligned}
& \begin{array}{c} k \\ \bullet \\ P_3 \end{array} \begin{array}{c} \Delta_1 \\ \bullet \\ \Delta_2 \end{array} \\
& \quad k - P_1 - P_2 \\
& = 3d_3 P_1 \cdot P_3 P_1 \cdot P_2 + 3d_4 P_2 \cdot P_3 P_1 \cdot P_2 \quad (51)
\end{aligned}$$

which again explicitly displays the color factor and where the new constants d_3 and d_4 have to be calculated in a specific model.

To reduce the ladder in this diagram we could attempt to use the Vector Ward Identity for the γ_μ on the left, but the momenta flowing in the adjoining propagators would require this γ_μ to be contracted with $-P_1 - P_2 = P_3 + P_4$ and not just with P_3 . Or in the right part of the diagram we could reuse our result for the two- Δ (\sqcup) vertex from the previous section. But again the momentum flow is not adequate. The solution to this impasse is to use both ideas, but in a momentum expansion. The ladder in this

diagram can be substituted by its momentum expansion (26). Since there are three powers of momentum already committed (one is the explicit P_3 , the other two need to be one in each Δ) only one more power is needed. Therefore we can use the ladder expansion to order one, and diagram (51) can be rewritten as

$$\begin{aligned}
 & \begin{array}{c} \text{Diagram 1: Ladder with two vertices and two external lines.} \\ O(P) \end{array} + \begin{array}{c} \text{Diagram 2: Ladder with two vertices and two external lines, with a loop.} \\ O(P^3) \end{array} \\
 & + \begin{array}{c} \text{Diagram 3: Ladder with two vertices and two external lines, with a loop and a vertex.} \\ O(P) \end{array} + \begin{array}{c} \text{Diagram 4: Ladder with two vertices and two external lines, with a loop and a vertex.} \\ O(P) \end{array} + \begin{array}{c} \text{Diagram 5: Ladder with two vertices and two external lines, with a loop and a vertex.} \\ O(P^2) \end{array}
 \end{aligned} \quad (52)$$

Now we can use the vector Ward-Takahashi Identity, which is satisfied to $O(P^{(1)})$, on the first diagram and on the left ladder of the second diagram, allowing us to substitute

$$P_3 \longrightarrow iS^{-1}(q) - iS^{-1}(q - P_3) .$$

The matrix object with a ladder and two deltas, to $O(P^{(2)})$, which appears on the second diagram, is just \square as defined in (42). Now it is straightforward to show that (51) is equal to

$$(2kP_3(A' \not{k} - B') + A \not{P}_3) \left(\begin{array}{c} \text{Diagram 1: Ladder with two vertices and two external lines.} \\ (q+P_1+P_2) \Delta_2 \end{array} + \begin{array}{c} \text{Diagram 2: Ladder with two vertices and two external lines.} \\ (q+P_1+P_2)^{(1)} \end{array} \right) \quad (53)$$

where the diagrams have to be evaluated to order $(P^{(3)})$ since an explicit power of P has already been used. The left diagram in particular gives rise to four simple sub-diagrams since two powers of P are committed in the Δ 's, but the other power can be distributed alternatively between these Δ 's or the two propagators which carry a power of P .

These diagrams can all be evaluated easily as a simple loop integral in the computer to obtain d_3, d_4 . The contribution from (47) is finally

$$\begin{aligned}
 & \frac{3}{(\sqrt{2}f_\pi)^4} (d_3(P_1 \cdot P_3 P_1 \cdot P_2 - P_1 \cdot P_2 P_2 \cdot P_3) \\
 & + d_4(P_2 \cdot P_3 P_1 \cdot P_2 - P_1 \cdot P_3 P_2 \cdot P_3) + \text{permutations}) \quad (54)
 \end{aligned}$$

D. Contribution with $\Delta\Gamma\Gamma\Gamma$.

The contribution

$$\begin{aligned}
 & \begin{array}{c} \text{Diagram 1: Ladder with two vertices and two external lines.} \\ \Gamma_4 \Delta_1 \end{array} + \begin{array}{c} \text{Diagram 2: Ladder with two vertices and two external lines.} \\ \Gamma_4 \Delta_1 \end{array} - \begin{array}{c} \text{Diagram 3: Ladder with two vertices and two external lines.} \\ \Gamma_4 \Delta_1 \end{array} \\
 & \begin{array}{c} \text{Diagram 4: Ladder with two vertices and two external lines.} \\ \Gamma_3 \Gamma_2 \end{array} \quad (55)
 \end{aligned}$$

can be reduced as follows: 1) apply (20) and (23) to the Δ_1 in the first term, and (12) to the Γ_3 in the second diagram to obtain an expression similar to (48) in which Γ_4 is isolated. 2) Employ (22) to eliminate Γ_4 . 3) Repeat the operation to eliminate Γ_2 . Obtain

$$\begin{aligned}
 & \begin{array}{c} \text{Diagram 1: Ladder with two vertices and two external lines.} \\ P_1 q P_3 \end{array} + \begin{array}{c} \text{Diagram 2: Ladder with two vertices and two external lines.} \\ q+P_1+P_4 \end{array} \\
 & \begin{array}{c} \text{Diagram 3: Ladder with two vertices and two external lines.} \\ P_1 q P_3 \end{array} + \begin{array}{c} \text{Diagram 4: Ladder with two vertices and two external lines.} \\ q+P_1+P_2 \end{array} \\
 & + \text{permutations} . \quad (56)
 \end{aligned}$$

In this expression, two explicit powers of P are present, namely P_1 and P_3 in the vertices. The other two powers have to be produced from a propagator expansion. This is the third (and last) different diagram type that we need to parameterize:

$$\begin{aligned}
 & \begin{array}{c} \text{Diagram 1: Ladder with two vertices and two external lines.} \\ P_1 q P_3 \end{array} + \begin{array}{c} \text{Diagram 2: Ladder with two vertices and two external lines.} \\ q+P_1+P_4 \end{array} \\
 & = 3d_5 P_1 \cdot P_3 P_1 \cdot P_4 + 3d_6 P_3 \cdot P_4 P_1 \cdot P_4 \quad (57)
 \end{aligned}$$

Next we show how to calculate d_5, d_6 . Since there is a ladder which contains powers of P , we need to recall the ladder expansion to second order in (26). Eliminating the loose rung with the help of (30), and employing the vector Ward Identity to generate a vertex

$$V(P) = 2q \cdot P(A'(q) \not{q} - B'(q)) + A(q) \not{P} ,$$

we can show

$$\begin{aligned}
 (57) = & \begin{array}{c} \text{Diagram 1: Ladder with two vertices and two external lines.} \\ V(P_1) \end{array} + \begin{array}{c} \text{Diagram 2: Ladder with two vertices and two external lines.} \\ V(P_3) \end{array} - \begin{array}{c} \text{Diagram 3: Ladder with two vertices and two external lines.} \\ V(P_1) \end{array} + \begin{array}{c} \text{Diagram 4: Ladder with two vertices and two external lines.} \\ V(P_3) \end{array} \\
 & \begin{array}{c} \text{Diagram 5: Ladder with two vertices and two external lines.} \\ (q+P_1+P_4)^{(2)} \end{array} + \begin{array}{c} \text{Diagram 6: Ladder with two vertices and two external lines.} \\ (q+P_1+P_4)^{(1)} \end{array} - \begin{array}{c} \text{Diagram 7: Ladder with two vertices and two external lines.} \\ (q+P_1+P_4)^{(1)} \end{array} + \begin{array}{c} \text{Diagram 8: Ladder with two vertices and two external lines.} \\ (q+P_1+P_4)^{(1)} \end{array} \quad (58)
 \end{aligned}$$

The first and third diagrams are again straightforward traces and integrals. Only the middle diagram contains

a ladder. We can interpret this ladder as “dressing” ei-

ther of the vertices, and write immediately an integral equation for one of them. Taking for example

$$[2kP_1(A'(k) \not{k} - B'(k)) + A(k) \not{P}_1] \text{ (diagram)} = \not{V} \quad (59)$$

(diagram: a square vertex with two external fermion lines on the left, one entering and one exiting, and two external fermion lines on the right, one entering and one exiting. The top-left line is labeled k and the bottom-left line is labeled $(k+P_1+P_4)^{(1)}$. The right side is labeled \not{V} .)

the function vertex \not{V} so defined satisfies a linear inhomogeneous integral equation (the first argument is the momentum entering the diagram through the vertex, the second is the relative and the third the total momentum between the fermion lines at the vertex):

$$\not{V}(P_1, k + \frac{P_1 + P_4}{2}, P_1 + P_4) = [2kP_1(A'(k) \not{k} - B'(k)) + A(k) \not{P}_1] S(k+P_1+P_4)^{(1)} S(k)^{-1} + \not{V} \text{ (diagram)} \quad (60)$$

(diagram: a square vertex with two external fermion lines on the left, one entering and one exiting, and two external fermion lines on the right, one entering and one exiting. The top-left line is labeled q and the bottom-left line is labeled q . The right side is labeled \not{V} .)

As is evident, \not{V} admits an expansion up to second order in momentum identical to (43) in terms of a new set of functions $\not{V}_0(k^2), \dots, \not{V}_9(k^2)$. The integral system of equations (60) is very similar to (44), the only difference being the inhomogeneous term. Therefore the linear projections in (45) still apply, and both systems can be solved with basically the same iterative computer code.

Finally the middle diagram in (58) can be closed to read

$$\not{V} \text{ (diagram)} = \not{V}(P_3) \text{ (diagram)} \quad (61)$$

(diagram: a square vertex with two external fermion lines on the left, one entering and one exiting, and two external fermion lines on the right, one entering and one exiting. The top-left line is labeled q and the bottom-left line is labeled $(q+P_1+P_4)^{(1)}$. The right side is labeled $\not{V}(P_3)$.)

which is easy to evaluate with the help of a symbolic manipulation program. Finally we give the expression for (55) in terms of the d 's:

$$3d_5 P_1 \cdot P_3 (P_1 \cdot P_4 + P_1 \cdot P_2) + 3d_6 (P_1 \cdot P_2 P_2 \cdot P_3 + P_1 \cdot P_4 P_3 \cdot P_4) + \text{permutations} . \quad (62)$$

E. Contribution with $\Delta\Delta\Gamma\Gamma$.

With two Δ corrections, there are two topologically distinct diagrams that can contribute. They are different because while reading around the fermion loop one can find the external legs in the order $\Gamma\Gamma\Delta\Delta$ or in the order $\Gamma\Delta\Gamma\Delta$. We start by the first term, namely

$$\text{(diagram 1)} + \text{(diagram 2)} - \text{(diagram 3)} \quad (63)$$

(diagram 1: a square vertex with two external fermion lines on the left, one entering and one exiting, and two external fermion lines on the right, one entering and one exiting. The top-left line is labeled Γ_4 and the bottom-left line is labeled Γ_3 . The right side is labeled Δ_1 and Δ_2 . Diagram 2: a square vertex with two external fermion lines on the left, one entering and one exiting, and two external fermion lines on the right, one entering and one exiting. The top-left line is labeled Γ_4 and the bottom-left line is labeled Γ_3 . The right side is labeled Δ_1 and Δ_2 . Diagram 3: a square vertex with two external fermion lines on the left, one entering and one exiting, and two external fermion lines on the right, one entering and one exiting. The top-left line is labeled Γ_4 and the bottom-left line is labeled Γ_3 . The right side is labeled Δ_1 and Δ_2 .)

(and the corresponding three more permutations). Again by applying (23) to the Δ_1 in the first diagram and (10)

to the Γ_3 in the second, then using (13) to simplify the remaining Γ_4 , neglecting the positive parity ladders when they are divided by a c_j containing the pion pole, reabsorbing the ladders and simplifying, one obtains:

$$\frac{P_3}{i} \text{ (diagram)} + \text{(diagram)} + \text{(diagram)} + \text{permutations} \quad (64)$$

(diagram 1: a square vertex with two external fermion lines on the left, one entering and one exiting, and two external fermion lines on the right, one entering and one exiting. The top-left line is labeled g and the bottom-left line is labeled $(q+P_3+P_4)$. The right side is labeled Δ_1 and Δ_2 . Diagram 2: a square vertex with two external fermion lines on the left, one entering and one exiting, and two external fermion lines on the right, one entering and one exiting. The top-left line is labeled g and the bottom-left line is labeled $(q+P_1+P_4)$. The right side is labeled Δ_1 and Δ_2 . Diagram 3: a square vertex with two external fermion lines on the left, one entering and one exiting, and two external fermion lines on the right, one entering and one exiting. The top-left line is labeled g and the bottom-left line is labeled $(q+P_1+P_4)$. The right side is labeled Δ_1 and Δ_2 .)

which can be written down immediately in terms of the d 's defined in eqns. (51), (57) as

$$3[-d_3 P_1 \cdot P_3 P_1 \cdot P_2 - d_4 P_2 \cdot P_3 P_1 \cdot P_2 + d_5 P_1 \cdot P_2 P_1 \cdot P_4 + d_6 P_2 \cdot P_4 P_1 \cdot P_4 + \text{permutations}] . \quad (65)$$

F. $\Delta\Gamma\Delta\Gamma$

Two permutations contribute: $\Delta_1\Gamma_2\Delta_3\Gamma_4$ and $\Gamma_1\Delta_2\Gamma_3\Delta_4$. The reduction is in all analogous to the previous ones, yielding a contribution

$$\frac{-3}{(\sqrt{2}f_\pi)^4} [d_5 (P_1 \cdot P_3 P_1 \cdot P_4 + P_1 \cdot P_3 P_3 \cdot P_4 + \text{permutation}) + d_6 (P_3 \cdot P_4 P_1 \cdot P_4 + P_1 \cdot P_4 P_3 \cdot P_4 + \text{permutation})] \quad (66)$$

G. $4 - \Gamma$ contribution.

The last piece stems from the term with four powers of Γ . By repeated use of (22) it can be shown to contribute

$$\frac{-3}{(\sqrt{2}f_\pi)^4} [d_5 (P_1 \cdot P_3 P_3 \cdot P_4 + P_1 \cdot P_3 P_2 \cdot P_3) + d_6 (P_1 \cdot P_4 P_3 \cdot P_4 + P_1 \cdot P_2 P_2 \cdot P_3)] . \quad (67)$$

(Here the cyclicity of (31) can be recovered by using $\sum_i P_i = 0$).

Combining the results from subsections A through F and summing all permutations (32) with the isospin factors (34, 35), the standard amplitude $A(s, t, u)$, takes a form identical to (4) and we deduce

$$l_1 = \frac{3}{32} (-2d_1 + d_2 - 6d_3 + 2d_4 + 5d_5 + d_6) \\ l_2 = -\frac{3}{16} (d_2 - 2d_3 + 2d_4 + d_5 - d_6) . \quad (68)$$

Therefore, to obtain the l 's numerically, one must:

1. Solve the Schwinger-Dyson equations for the propagator, equation (7).

2. Employ the obtained A , B functions as input to the Bethe-Salpeter equations (16) and solve them.
3. Then use the obtained F_0 , G_0 , ... as input for equations (44) and (60) to obtain \sqcup and \sqcup .
4. Perform the integrals (46), (53), (61).
5. Assemble (40), (54), (62), (65), (66), (67).

In this external momentum expansion all integrals and integral equations are functions of internal variables only of quark momenta q^2 , k^2 , $k \cdot q$. The diagrams could alternatively be evaluated on the lattice.

V. MODEL EVALUATIONS.

We would like to provide simple model evaluations of all these calculations, well aware of model limitations and that a thorough phenomenological analysis can only be carried out with more sophisticated interactions such as employed in [7, 12]. We employ two Feynman gauge models featuring an interaction

$$VK(q)V = \gamma_\mu K(q) \gamma^\mu. \quad (69)$$

This simple choice of a vector-vector interaction (as opposed to the more popular Landau gauge transverse tensor kernel) simplifies the Gamma matrix traceology (in this calculation carried out with the help of two independent computer codes, one written in MATHEMATICA and one in FORM [22]) so that the standard Llewellyn-Smith BS wavefunction for the pion [7] reduces to

$$\chi(P, k) = \gamma_5 (E(P, k) + F(P, k) \not{P} + G(P, k) \not{k} k \cdot P)$$

$$= \gamma_5 \left(E0(k^2) + \frac{(kp)^2}{2} E2(k^2) + F0(k^2) \not{P} + G0(k^2) \not{k} k \cdot P + \dots \right) \quad (70)$$

where the standard H function decouples from the rest of the system and therefore we further ignore, and the momentum expansion shown is complete up to second order for a symmetric momentum routing χ (that is, the fermion lines out of χ carry $k + P/2$ and $k - P/2$). The $E0$ term is determined by chiral symmetry to be $\frac{\Gamma_A(P=0, k)}{\sqrt{2}if_\pi}$. The rest of the expansion constructs the function $\Delta(P, k)$. The same power series (70) can be written down for the axial vertex,

$$\Gamma_A(P, q) = [(A(q - P/2)(\not{q} - \frac{\not{P}}{2}) - A(q + P/2)(\not{q} + \frac{\not{P}}{2}) - (B(q - P/2) + B(q + P/2))\gamma_5] \gamma_5 \quad (71)$$

expanding in powers of P , and up to a normalization we recover the equivalent to (70)

$$\begin{aligned} E0_A &= 2B(q^2) \\ F0_A &= -A(q^2) \\ G0_A &= -2A'(q^2) \\ E2_A &= 2B''(q^2) \\ &\dots \end{aligned} \quad (72)$$

Subtracting (72) from (70) we obtain some new functions of q^2 which provide the needed expansions for Δ :

$$\begin{aligned} \Delta^{(1)}(q + P_1/2, P_1) &= \Delta^{(1)}(q, P_1) = \overline{F0}(q^2) \not{P}_1 + \overline{G0}(q^2) q \cdot P_1 \not{q} \\ \Delta^{(2)}(q + P_1/2, P_1) &= E^2(q^2) \frac{(q \cdot P_1)^2}{2} + \overline{F0}'(q^2) \not{P}_1 q \cdot P_1 + \overline{G0}'(q^2) \not{q} (q \cdot P_1)^2 \end{aligned} \quad (73)$$

(valid for symmetric momentum routing when $E1$, $F1$, $G1$ all vanish). Further, with the $\gamma_\mu \gamma^\mu$ kernel another trace-related simplification occurs in (44) and (60), and the functions \sqcup_6 , \sqcup_7 , \sqcup_8 , \vee_6 , \vee_7 , \vee_8 equal the inhomogeneous term in their respective equations, the homogeneous (integral) parts of the equations being zero.

All that remains is to consider some specific form for $K(q^2)$. We will look at two models whose euclidean angular integrals can be done analytically, leaving only one-dimensional integral equations to solve numerically.

The first is a simple Gaussian kernel (whose Euclidean angular integrals are Bessel functions [23])

$$K(q) = g^2 \exp(-q^2/\Lambda^2) \quad (74)$$

where g provides the coupling strength and Λ the scale of the interaction. (the results are sketched in table I).

The second is a rational kernel

$$K(q) = g^2 [1/(q^2 - \lambda^2) - 1/(q^2 - \Lambda^2)] \quad (75)$$

where g , λ and Λ represent some quark model parameters fit to provide a good condensate and constituent quark mass via the Schwinger-Dyson equation. The euclidean angular integrals are straight-forward using relations such as

$$\int_{-1}^1 \frac{\sqrt{1-x^2}}{a-x} = \pi(a - \sqrt{a^2-1}),$$

TABLE I: Results for the toy gaussian model in the chiral limit. Dimensionful magnitudes are in MeV.

Λ	g	$M(k^2 = 0)$	$-\langle\bar{\Psi}\Psi\rangle^{1/3}$	f_π	l_1	l_2
500	6.3	385	222	76	-0.02	0.066
600	6.3	462	267	91	-0.02	0.060
500	6.5	468	237	83	-0.018	0.062
800	5.5	125	213	51	-0.019	0.080

TABLE II: Results for the toy rational model in the chiral limit. Dimensionful magnitudes are in MeV.

λ	Λ	g	$M(k^2 = 0)$	$-\langle\bar{\Psi}\Psi\rangle^{1/3}$	f_π	l_1	l_2
250	300	13.0	559	242	82	-0.011	0.11
300	350	13.0	471	240	77	-0.015	0.11
500	550	14.2	269	247	68	-0.015	0.12
700	770	13.4	155	250	56	-0.012	0.12

$$\int_{-1}^1 \frac{x\sqrt{1-x^2}}{a-x} = \pi(a^2 - 1/2 - a\sqrt{a^2 - 1}) .$$

Hence all integral equations are one-dimensional in momentum space.

When the dimensionful parameters, of order the strong interaction scale, are close in value, and for large enough g , then the potential is infrared enhanced supporting chiral symmetry breaking. Notice that the Rainbow-Ladder fermion loop diagrams constructed with these interactions are finite due to the exponential or $1/q^4$ high energy behavior and no renormalization program is needed. This is associated to a gluon propagator scale, which determines the scale of the Bethe-Salpeter wavefunctions, which in turn regulate the meson loops that would appear in chiral perturbation theory. We are currently investigating this issues.

VI. RESULTS AND DISCUSSION

We have worked out the pion-pion scattering amplitude at low energy in the chiral limit to $O(P^4)$ from a general microscopic quark Schwinger-Dyson approach. Upon comparison with the chiral lagrangian formalism, the main result of this paper is a pair of relations that would in principle allow to directly evaluate the coefficients l_1 , l_2 in any specific model (i.e. after choosing the Lorentz structure of the quark-antiquark interaction, strength and shape of any potential or dressed gluon propagator) provided it supports the standard mechanism of chiral symmetry breaking [17], [18], [24]. symmetry properties of the Γ pion vertex, are model dependent and are of order P^4 (therefore vanishing at low energy). Lorentz invariance restricts their form and allows only for two coefficients.

On a first glance, diagrams (40, etc.) seem as difficult

to calculate as the full pion-pion scattering amplitude, but one needs to remember that each Δ pion wavefunctions entering the calculation can be taken to have only one power of the external P to this order, since there are four of them and they vanish by definition at $P = 0$, and the propagators can also be taken at $P = 0$, leaving just one momentum k around the loop. This is a major simplification.

In the previous section we have shown how the numerical evaluation can be performed with two very simple (too simple) kernels. Our results for l_1 and l_2 have phenomenologically correct signs and ratios, specially for the gaussian toy model, see tables I and II. Possibly because our results are computed at $P = 0$ and without pion loops, our l_1 and l_2 seem too large in absolute value. This can be appreciated [4, 6, 9, 10, 21, 25, 26, 27, 28, 29, 31] in tables III, IV and V which summarize the present status of knowledge of these coefficients. The various conventions used in the literature ($SU(3)$, $SU(2)$, renormalized, barred, etc.) have been unified to the renormalized l 's at the scale of the ρ meson. Some of those determinations carry information relative to finite quark (and therefore pion) masses, to kaons and etas, or to pion loops, all of which have not been taken into account in this work. The fairest comparison therefore is with the oldest results of Andrianov [10] in the large N_c limit (no gluon corrections) and Pham and Truong [27]. The later authors obtain the interesting relations

$$l_2 = \frac{f_\pi^2}{m_\rho^2}$$

and

$$l_1 = \frac{1}{3} \frac{f_\pi^2}{m_\sigma^2} - 2l_2 .$$

If the σ mass is sent to infinity, then the large N_c ratio is recovered. For finite σ masses between 350 and 750 MeV we obtain the range given in table IV. This demonstrates the importance of repeating the model evaluations with kernels whose meson excitations in various channels are known.

Our approach is potentially superior to the resonance saturation approximations since it includes the full vertex and ladder structures, that is, effects of continua and higher resonances. In particular we include the four pion direct interaction, and the exchange of the full series of excited vector and scalar mesons. We also stress that the masses of our ρ and σ mesons are expected to be of the right order of magnitude, because our constituent quark mass have reasonable values of the order of $300MeV$ to $400MeV$, see tables I and II. Our approach is also potentially superior to Nambu-Jona-Lasinio determinations by allowing to lift the approximation of contact interactions between quarks. Thus we pave the way to calculating the l_i coefficients from the lattice or from accurate Schwinger-Dyson solutions. Finite current quark masses and meson loops remain to be incorporated to improve the precision

of our calculation. We are currently considering some of these issues.

TABLE III: Phenomenological determinations of the l parameters (fits to scattering lengths or phase shifts in pion scattering.)

Authors	$l_1^r(m_\rho) \cdot 10^3$	$l_2^r(m_\rho) \cdot 10^3$
Gasser & Leutwyler	-4.2 ± 3.9	9.0 ± 2.7
Bijnens, Colangelo, Talavera;		
Colangelo, Gasser, Leutwyler	-2.2 ± 0.6	9.0 ± 2.7
Yndurain	-4.1 ± 0.7	9.8 ± 0.5
Gómez Nicola & Peláez	-3.3 ± 0.7	4.8 ± 0.6

TABLE IV: Phenomenological determinations of the l parameters (Based on ρ meson resonance saturation).

Authors	$l_1^r(m_\rho) \cdot 10^3$	$l_2^r(m_\rho) \cdot 10^3$
Gasser & Leutwyler	-8.4	8.4
Pham & Truong	-5.5 to -24	14
Ecker <i>et al.</i>	-6.1 ± 3.9	5.3 ± 2.7
Pennington & Portolés	-2.1 ± 1.2	5.9 ± 1.0

TABLE V: Theoretical determinations of the l parameters (based on the large N_c approximation and/or the Nambu-Jona-Lasinio model).

Authors	$l_1^r(m_\rho) \cdot 10^3$	$l_2^r(m_\rho) \cdot 10^3$
Espriu, de Rafael, Taron	-3.18	6.3
Bijnens, Bruno, de Rafael	-4.8	6.4
Ruiz Arriola	-7.4	7.8
Andrianov	-3.2	6.4

Acknowledgments

The authors acknowledge useful discussions with S. Cotanch, F. Kleefeld, B. Hiller, P. Maris, J. R. Peláez, A. Dobado, A. Gomez Nicola and specially E. Ribeiro. Work partially supported by univ. Complutense on a travel grant, and by grants FPA 2000-0956, BFM 2002-01003 (Spain), F. J. Llanes-Estrada is thankful for the hospitality and scholarly atmosphere at IST Lisbon.

-
- [1] Fritz London, Z. Physik **63**, 245 (1930).
 - [2] M. M. Nagels, T. A. Rijken, and J. J. de Swart, Phys. Rev. **D 17**, 768 (1978).
 - [3] R. B. Wiringa, V. G. J. Stoks and R. Schiavilla, Phys. Rev. **C 51**, 38 (1995).
 - [4] J. Gasser and H. Leutwyler, Ann. Phys. **158**, 142 (1984). J. Gasser and H. Leutwyler, Nucl. Phys. **B 250**, 465 (1985).
 - [5] B. Renner, “Current Algebras and their Applications”, Pergamon Press (1968).
 - [6] J. A. Oller, E. Oset, J. R. Peláez, Phys. Rev. **D 59**, 074001 (1999); *id.* Phys. Rev. Lett. **80**, 3452 (1998); A. Gomez Nicola and J. R. Peláez, Phys. Rev. **D 65**:054009 (2002).
 - [7] P. Maris and C. D. Roberts, Phys. Rev. **C 56**, 3369 (1997). P. Maris, C. D. Roberts and P. C. Tandy, Phys. Lett. **B 420**, 267 (1998).
 - [8] J. Alfaro, A. Dobado, D. Espriu, Phys. Lett. **B 460**, 447 (1999).
 - [9] J. Bijnens, C. Bruno and E. de Rafael, Nucl. Phys. **B 390**, 501-541 (1993). E. Ruiz Arriola, Phys. Lett. **B 253**, 430 (1991).
 - [10] A. A. Andrianov, Phys. Lett. **B 157**, 425 (1985).
 - [11] D. R. Nelson, G. T. Fleming and G. W. Kilcup, Phys. Rev. Lett. **90**:021601 (2003).
 - [12] C. D. Roberts *et al.* Phys. Rev. **D 49**, 125 (1994). See also C. D. Roberts, R. T. Cahill, J. Praschifka, Ann. Phys. **188**, 20 (1988).
 - [13] P. de A. Bicudo *et al.* Phys. Rev. **D 65**: 076008 (2002).
 - [14] P. Bicudo, Phys. Rev. **C 67**, 035201 (2003); P. Bicudo, in *Quark Confinement and the Hadron Spectrum V*, World Scientific, ed. N. Brambilla and G. Prosperi (2002) [arXiv:nucl-th/0110052].
 - [15] S. R. Cotanch and P. Maris, Phys. Rev. **D 66**, 116010 (2002) [arXiv:hep-ph/0210151].
 - [16] H. Lehman, Phys. Lett. **B 41**, 529 (1972); *id.* Acta Phys. austriaca suppl. **11**, 139 (1973).
 - [17] P. de A. Bicudo and J. E. F. T. Ribeiro, Phys. Rev. **D 42**, 1611 (1990); *id.* Phys. Rev. **D 42**, 1625 (1990); *id.* Phys. Rev. **D 42**, 1635 (1990).
 - [18] A. Le Yaouanc *et al.* Phys. Rev. **D 31**, 137 (1985).
 - [19] Y. Dai, C. Huang, D. Liu Phys. Rev. **D 43**, 1717 (1991); J. E. Villate, *et al.*, Phys. Rev. **D 47**, 1145 (1993).
 - [20] R. Delbourgo and M. D. Scadron, J. Phys. **G 5**, 1621 (1979).
 - [21] G. Ecker, J. Gasser, A. Pich, E. de Rafael, Nucl. Phys. **B 321**, 311 (1989). J. J. Sanz-Cillero and A. Pich, hep-ph/0208199 preprint.
 - [22] J. A. M. Vermaseren “New Features of Form”, math-ph/0010025 preprint.
 - [23] R. Alkofer, P. Watson and H. Weigel Phys. Rev. **D 65**:094026 (2002).
 - [24] F. J. Llanes-Estrada and S. R. Cotanch, Nucl. Phys. **A 697**, 303 (2002); *id.* Phys. Rev. Lett. **84**, 1102 (2000).
 - [25] M. R. Pennington, J. Portolés, Phys. Lett. **B 344**, 399 (1995).
 - [26] J. Bijnens, G. Colangelo, P. Talavera, JHEP 9805:014 (1998); G. Colangelo, J. Gasser, H. Leutwyler, Nucl. Phys. **B 603**, 125 (2001).
 - [27] T. N. Pham and Tran N. Truong, Phys. Rev. **D 31**, 3027 (1985).
 - [28] F. J. Yndurain, “Low Energy Pion Physics”,

hep-ph/0212282.

- [29] D. Espriu, E. de Rafael and J. Taron, Nucl. Phys. **B 345**:22-56 (1990).
 [30] C. H. Llewellyn Smith, Nuovo Cimento **LX**, 348 (1969).
 [31] E. Ruiz Arriola, Phys. Lett. **B 253**, 430 (1990).
 [32] A short preliminary version of this work has been reported in the Vth International Conference on Quark Confinement and the Hadron Spectrum, see preprint hep-ph/0212182 by F. J. Llanes-Estrada and P. Bicudo.

APPENDIX A: NORM AND f_π

In this appendix we present the proof of the well known fact that the normalization of the Bethe-Salpeter wavefunction is the pion decay constant, rewritten in terms of our Ward Identity techniques. At null external pion momentum, $\chi^a(P=0)$ and Γ_A^a are proportional because eq. (10) reduces to the homogeneous BS eq. (16). Introduce an arbitrary proportionality constant n_π by means of

$$\chi^a(P=0) = \frac{\Gamma_A^a}{in_\pi} ; \quad (A1)$$

the i guarantees χ to be real because of the explicit form of Γ in eq. (18).

The normalizing condition for the Bethe-Salpeter solution is, following Llewellyn-Smith [30],

$$\chi_{-P}^a \circlearrowleft \frac{\partial}{\partial P^\mu} \left(\begin{array}{c} \rightarrow \\ \rightarrow \end{array} \right) \circlearrowright \chi_P^b = 2i P_\mu \delta^{ab} . \quad (A2)$$

Because the right hand side of the normalization condition is of first order in P^μ we can expand in χ and in Γ_A as in (20). There are two terms, depending on whether the derivative is applied to the upper or lower propagator.

The first term can be written as

$$\begin{aligned} & \chi_{-P}^a \circlearrowleft \frac{\partial}{\partial P^\mu} \left(\begin{array}{c} \rightarrow \\ \rightarrow \end{array} \right) \circlearrowright \chi_P^b = - \frac{\Gamma_{A-P}^a \circlearrowleft \begin{array}{c} \partial_\mu S^{-1} \\ \rightarrow \end{array} \circlearrowright \Gamma_{A-P}^b}{(in_\pi)^2} \\ & + \frac{\Gamma_{A-P}^a \circlearrowleft \begin{array}{c} \partial_\mu S^{-1} \\ \rightarrow \end{array} \circlearrowright \chi_P^b}{in_\pi} + \frac{\chi_{-P}^a \circlearrowleft \begin{array}{c} \partial_\mu S^{-1} \\ \rightarrow \end{array} \circlearrowright \Gamma_{A-P}^b}{in_\pi} \end{aligned} \quad (A3)$$

The term with $\Gamma\Gamma$ can be shown to be zero. To see it, one needs to take a derivative of eq. (7) which gives

$$S \partial_\mu S^{-1} S = \begin{array}{c} \rightarrow \\ \rightarrow \end{array} \begin{array}{c} \rightarrow \\ \rightarrow \end{array} \begin{array}{c} \rightarrow \\ \rightarrow \end{array} \partial_\mu S_0^{-1} \quad (A4)$$

which applied to the $\Gamma\Gamma$ term in (A3) and employing eq. (22) reduces it to

$$-\Gamma_{A-P}^a \circlearrowleft \begin{array}{c} \partial_\mu S^{-1} \\ \rightarrow \end{array} \circlearrowright \Gamma_{A-P}^b = -\gamma_{A-P} \frac{\sigma^a}{2} \begin{array}{c} \rightarrow \\ \rightarrow \end{array} \begin{array}{c} \rightarrow \\ \rightarrow \end{array} \begin{array}{c} \rightarrow \\ \rightarrow \end{array} \begin{array}{c} \partial_\mu S_0^{-1} \\ \rightarrow \end{array}$$

$$= -\gamma_{5-P} \gamma_A \begin{array}{c} \rightarrow \\ \rightarrow \end{array} \begin{array}{c} \rightarrow \\ \rightarrow \end{array} \begin{array}{c} \rightarrow \\ \rightarrow \end{array} \begin{array}{c} \partial_\mu S^{-1} \\ \rightarrow \end{array} + -\Gamma_A \begin{array}{c} \rightarrow \\ \rightarrow \end{array} \begin{array}{c} \rightarrow \\ \rightarrow \end{array} \begin{array}{c} \rightarrow \\ \rightarrow \end{array} \begin{array}{c} \partial_\mu S_0^{-1} \\ \rightarrow \end{array} \gamma_{5-P} \quad (A5)$$

re-absorbing the remaining ladder, and employing the free propagator and bare axial vertex in eq. (5, 9) this is proportional (because of the isospin factor not included) to

$$Tr \int (i \not{P} S \partial_\mu S^{-1} S - \Gamma_{A-P} S \frac{\gamma_\mu \gamma_5}{2i} S) . \quad (A6)$$

Eliminating Γ with its Ward Identity (13), and after some elementary operations, this equals

$$-i Tr (\gamma_\nu \partial_\mu S - \partial_\nu S \gamma_\mu) P_\nu = 0 . \quad (A7)$$

Returning to equation (A3) and once the term with $\Gamma\Gamma$ has been shown to vanish, we need to evaluate the terms with a χ and a Γ .

Diagrammatically again, one has (recall equations (22), (23) and (A4))

$$\begin{aligned} & \Gamma_{A-P}^a \circlearrowleft \begin{array}{c} \partial_\mu S^{-1} \\ \rightarrow \end{array} \circlearrowright \chi_P^b \\ & \frac{\chi_P^b}{c} \begin{array}{c} \rightarrow \\ \rightarrow \end{array} \begin{array}{c} \rightarrow \\ \rightarrow \end{array} \begin{array}{c} \rightarrow \\ \rightarrow \end{array} \begin{array}{c} \Gamma_A^a \\ \rightarrow \end{array} \begin{array}{c} \rightarrow \\ \rightarrow \end{array} \begin{array}{c} \rightarrow \\ \rightarrow \end{array} \begin{array}{c} \partial_\mu S_0^{-1} \\ \rightarrow \end{array} \\ & = \gamma_5 \frac{\sigma^a}{2} \frac{\chi_P^b}{c} \begin{array}{c} \rightarrow \\ \rightarrow \end{array} \begin{array}{c} \rightarrow \\ \rightarrow \end{array} \begin{array}{c} \rightarrow \\ \rightarrow \end{array} \begin{array}{c} \partial_\mu S^{-1} \\ \rightarrow \end{array} \\ & + \chi_P^b \begin{array}{c} \rightarrow \\ \rightarrow \end{array} \begin{array}{c} \rightarrow \\ \rightarrow \end{array} \begin{array}{c} \rightarrow \\ \rightarrow \end{array} \begin{array}{c} \partial_\mu S_0^{-1} \\ \rightarrow \end{array} \gamma_{5-P} \frac{\sigma^a}{2} \\ & = -\frac{1}{c} Tr \{ \gamma_{5-P} \frac{\sigma^a}{2} \chi_P^b \partial_\mu S(k+P/2) \} \\ & + \frac{1}{2i} \chi_P^b \begin{array}{c} \rightarrow \\ \rightarrow \end{array} \begin{array}{c} \rightarrow \\ \rightarrow \end{array} \begin{array}{c} \rightarrow \\ \rightarrow \end{array} \gamma_\mu \gamma_5 \frac{\sigma^a}{2} . \end{aligned} \quad (A8)$$

We get two terms. The first is of order P^2 because of the c in the denominator, and vanishes. The second is indeed non zero. Going back now to eq. (A2), we obtain

$$2i P_\mu = \left(\frac{1}{in_\pi} 2i \right) \chi_P^b \begin{array}{c} \rightarrow \\ \rightarrow \end{array} \begin{array}{c} \rightarrow \\ \rightarrow \end{array} \begin{array}{c} \rightarrow \\ \rightarrow \end{array} \gamma_5 \gamma_\mu \frac{\sigma^a}{2} \quad (A9)$$

The definition of the weak decay constant, f_π yields (with no pion loops)

$$\chi_P^b \begin{array}{c} \rightarrow \\ \rightarrow \end{array} \begin{array}{c} \rightarrow \\ \rightarrow \end{array} \begin{array}{c} \rightarrow \\ \rightarrow \end{array} \gamma_5 \gamma_\mu \frac{\sigma^a}{2} = i P_\mu f_\pi \delta^{ab} \quad (A10)$$

and therefore we must have

$$n_\pi = f_\pi$$

which immediately leads to equation (20). Finally, direct calculation of equation (A10) leads to

$$if_\pi^2 = 3 \int \frac{d^4 q}{(2\pi)^4} \frac{1}{(A^2 q^2 - B^2)^2} \left[E0 \left(4AB + 2q^2 \left(B \frac{dA}{d(q^2)} - A \frac{dB}{d(q^2)} \right) \right) + F0(2q^2 A^2 + 4B^2) + q^2 G0(B^2 - q^2 A^2) \right]. \quad (\text{A11})$$

Notice the explicit color factor of 3. All through the paper the Bethe-Salpeter wavefunctions have been taken proportional to the identity $\delta_{cc'}$ in color space. Had we normalized them in a different way, say $\delta_{cc'}/\sqrt{3}$, this would immediately affect the formula above reducing the factor to $\sqrt{3}$, the rest being absorbed by the functions $E0$, $F0$, $G0$. The low energy theorems (Gell-Mann-Oakes-Renner theorem, Weinberg's amplitude, etc.) are unchanged by this choice since the explicit form of these functions is never used to prove them: they are always eliminated in terms of f_π . But the l_1 , l_2 constants of the chiral lagrangian would indeed have to be rewritten in terms of the modified Bethe-Salpeter wavefunctions. This of course would not affect its numerical value.

The normalizing condition (A2),

$$\chi_{-P} \circlearrowleft \frac{\partial}{\partial P^\mu} \left(\begin{array}{c} \overrightarrow{\quad} \\ \overleftarrow{\quad} \end{array} \right) \circlearrowright \chi_P = 2i P_\mu. \quad (\text{A12})$$

which yields (A10) can also be directly evaluated without using Ward Identities. By taking a derivative of this equation respect to P^μ (and contracting over μ as usual), we get the following (derivatives respect to P act only on the function immediately behind them and the color

factor is explicit).

$$8i = 3 \int \frac{d^4 q}{(2\pi)^4} \text{Tr} [\quad (\text{A13})$$

$$\begin{aligned} & 2\partial_\mu \chi_\pi(P) \partial^\mu S(q + P/2) \chi_\pi(-P) S(q - P/2) + \\ & 2\chi_\pi(P) \partial_\mu \partial^\mu S(q + P/2) \chi_\pi(-P) S(q - P/2) + \\ & 2\chi_\pi(P) \partial_\mu S(q + P/2) \partial^\mu \chi_\pi(-P) S(q - P/2) + \\ & 2\chi_\pi(P) \partial^\mu S(q + P/2) \chi_\pi(-P) \partial_\mu S(q - P/2) + \end{aligned}$$

To calculate this normalization one needs to make the wavefunction explicit

$$\chi_\pi(P) = \gamma_5 (E0(q^2) + F0(q^2) \not{P} + G0(q^2) q \cdot \not{q} + \dots) \quad (\text{A14})$$

which evaluated at $P = 0$ yields

$$\chi_\pi(0) = \gamma_5 E0(q^2); \quad \partial_\mu^P \chi_\pi(P=0) = \gamma_5 (F0 \gamma_\mu + G0 \not{q}_\mu).$$

and make use of the propagator expansion, (27, 28, 29) above. A simple check on the resulting expression is to substitute χ by Γ , which yields

$$-3 \int \frac{d^4 q}{(2\pi)^4} \left[-2B(\partial_\rho B) \partial^\rho \left(\frac{1}{A^2 q^2 - B^2} \right) - B^2 \partial_\rho \partial^\rho \left(\frac{1}{A^2 q^2 - B^2} \right) \right] = 0$$

which vanishes upon employing Green's first identity. This checks the zero in (A7) with a completely independent calculation, and is also approximately observed in our computer codes. The result for n_π is

$$n_\pi^2 = 3i \int \frac{d^4 q}{(2\pi)^4} \frac{1}{A^2 q^2 - B^2} [(AB' - BA') 2q^2 B(\overline{F}_0 + q^2 \overline{G}_0) \quad (\text{A15})$$

$$-AB^2(4\overline{F}_0 + q^2 \overline{G}_0)] \quad (\text{A16})$$

which, upon comparison with. (A11) provides an integral constraint between the Schwinger-Dyson and Bethe-Salpeter solutions. The barred quantities have been defined in (73).

To conclude this discussion we recall the derivation of the Gell-Mann-Oakes-Renner relation in the Bethe-Salpeter formalism. this has been presented in [13], [14], together with the discussion of the Weinberg theorem. At zero external pion momentum the Axial Ward Identity reads

$$2im\Gamma_5^a(k, k) = \frac{\sigma^a}{2} (\gamma_5 S^{-1} + S^{-1} \gamma_5) \quad (\text{A17})$$

and as previously discussed

$$\Gamma_5^a = \frac{B_k}{m} \frac{\sigma^a}{2} \gamma_5 \quad (\text{A18})$$

To start the simple demonstration of GMOR, "undress" the vertex Γ_5^a to write

$$S \Gamma_5^a S = \begin{array}{c} \text{---} \rightarrow \text{---} \\ \text{---} \rightarrow \text{---} \end{array} \begin{array}{c} \text{---} \rightarrow \text{---} \\ \text{---} \rightarrow \text{---} \end{array} \gamma_5 \frac{\sigma^a}{2} \quad (\text{A19})$$

and, neglecting the contribution of higher pion states (which exactly decouple in the chiral limit, as in ref. [24]) we can saturate the ladder by the pion pole yielding

$$\Gamma_5^a \simeq \gamma_5 \frac{\sigma^a}{2} \text{---} \text{---} \text{---} \chi^a \frac{i}{P^2 - M_\pi^2} \chi^a \quad (\text{A20})$$

substituting now eq. (A1) in the form

$$\chi^a = \frac{S^{-1} \gamma^5 + \gamma^5 S^{-1}}{i n_\pi} \frac{\sigma^a}{2} \quad (\text{A21})$$

and comparing with eq. (A18) we immediately obtain

$$-2m \text{Tr} S = n_\pi^2 M_\pi^2$$

corresponding to the GMOR relation upon identification of $n_\pi = f_\pi$, consistent with the Llewellyn-Smith normalization condition.

We finally remind the reader of the explicit expression for the BCS planar condensate:

$$\begin{aligned} \langle \bar{\Psi}_u \Psi_u \rangle &= \langle \bar{\Psi}_d \Psi_d \rangle = \text{Tr} S = \\ i \text{Tr} \int &\frac{A_k \not{k} + B_k}{A_k k^2 - B_k^2 + i\varepsilon} = \\ -3 \int &\frac{d^4 k_E}{(2\pi)^4} \frac{4B_k}{A_k^2 k^2 + B_k^2} \end{aligned} \quad (\text{A22})$$